

First-principles scattering with Büttiker probes: The role of self-energiesAlexander Fabian,^{1,2,*} Martin Gradhand,^{3,4} Michael Czerner,^{1,2} and Christian Heiliger^{1,2}¹*Institute for Theoretical Physics, Justus-Liebig-University Giessen, Heinrich-Buff-Ring 16, 35392 Giessen, Germany*²*Center for Materials Research (LaMa), Justus-Liebig-University Giessen, Heinrich-Buff-Ring 16, 35392 Giessen, Germany*³*HH Wills Physics Laboratory, University of Bristol, Tyndall Avenue BS8 1TL, United Kingdom*⁴*Institute of Physics, Johannes Gutenberg University Mainz, 55099 Mainz, Germany*

(Received 1 November 2021; revised 28 February 2022; accepted 29 March 2022; published 5 April 2022)

Understanding electronic transport properties is important for designing devices for applications. Many studies rely on the semiclassical Boltzmann approach within the relaxation time approximation. This method delivers a graphic physical picture of the scattering process, but in some cases it lacks full quantum-mechanical effects. Here, we use a non-equilibrium Green's function Korringa-Kohn-Rostoker (KKR) method with phase-breaking scattering via virtual Büttiker terminals as a fully quantum mechanical approach to transport phenomena. With this, we assess the validity of the relation of the self-energy Σ to the scattering time τ , often used in literature in the case of constant relaxation time approximation. We argue that the scattering time does not affect the thermopower in the Boltzmann approach and thus should take no effect either on the thermopower calculated via the Keldysh approach. We find a nearly linear relation for the transmission function $T_S(E_F, \Sigma)$ of free electrons and Cu with respect to $\frac{1}{\Sigma}$. However, we find that this is not the case for Pd. We attribute this to neighboring states contributing due to the additional broadening via the self-energy Σ . These findings suggest that a simple identification of scattering time and self-energy is not sufficient. Finally, we discuss the benefits and limits of the application of the virtual terminal approach.

DOI: [10.1103/PhysRevB.105.165106](https://doi.org/10.1103/PhysRevB.105.165106)**I. INTRODUCTION**

In the past years, electronic devices have become significantly smaller. Further shrinking the sizes leads to quantum mechanical effects that dominate the transport properties [1–4]. There are several approaches from classical to fully quantum mechanical to characterize transport quantities. Scattering can be accounted for in each of these approaches and of course, the type of scattering has huge influences on the transport properties. While there are full quantum mechanical formalisms like the Kubo formalism [5–9] or the steady-state Keldysh [10–12] formalism, often semiclassical approaches are used to describe transport properties. The physical picture in these semiclassical approaches, mainly the Boltzmann formalism [13–17], is quite intricate since it enables an intuitive understanding in terms of scattering processes. One of the principal quantities for understanding this scattering picture is the scattering or relaxation time τ , which gives the mean time between two scattering events.

Often, first-principle methods rely on the averaging over many configurations of lattice distortions or impurities to obtain semiclassical like features [18,19]. However, room temperature like features can also be established by introducing a dephasing mechanism by means of Büttiker probes (or virtual terminals) [20,21]. In our purely quantum-mechanical Keldysh approach including dephasing virtual terminals, it

is not the scattering time, which is the primary determining quantity, but a broadening of the states given by the negative imaginary part Σ of the complex self-energy $\bar{\Sigma}$, which is often directly related to the scattering time in angle-resolved photoemission spectroscopy (ARPES) experiments [22,23]. In such scenarios the scattering time is often identified with the lifetime of the state, $\tau_{\text{scat}} = \tau_{\text{life}} = \frac{\hbar}{2\Sigma}$ [24]. For ARPES experiments it was discussed that the single-particle lifetime can be related to the self-energy in this way, but that this single-particle lifetime differs from the lifetime of an excited photoelectron population [25]. The discrepancies were supported by experimental findings [26–28]. Hence, a simple identification of scattering time and self-energy seems nontrivial. However, even in a single-particle description, this simple relationship between lifetime and self-energy might fail.

In this paper, we test the relation of the scattering time and the scattering self-energy in a single-particle description but for real materials. We give an example where such a direct identification is questionable, even for simple, pure metals. This is shown by comparing the theory of the Boltzmann approach with results from a Keldysh non-equilibrium Green's function approach [11,29] in the framework of a Korringa-Kohn-Rostoker (KKR) [30] density functional theory (DFT), in which we use virtual terminals (also known as Büttiker probes) to describe incoherent elastic scattering [10]. We discuss the limit of applicability of virtual terminals by comparing the results of the KKR implementation with a simple finite differences method (FDM) for the case of free electrons [29].

*Alexander.Fabian@physik.uni-giessen.de

II. THEORY

In order to evaluate transport properties, the following moments L_n are used [31]:

$$L_n = \frac{2}{h} \int dE \int d\vec{k}_{\parallel} (E - \mu)^n \left(-\frac{\partial f(E, \mu, \theta)}{\partial E} \right) T(E, \vec{k}_{\parallel}), \quad (1)$$

where h is Planck's constant, E is the energy, μ is the chemical potential, θ the temperature, $f(E, \mu, \theta)$ is the Fermi-Dirac distribution, and $T(E, \vec{k}_{\parallel})$ the $\vec{k}_{\parallel} = (k_x, k_y)$ dependent transmission function. Normally, these moments are written as tensors. Here, since we are looking at cubic systems only, we restrict ourselves to the $L_n = L_{n,zz}$ component of the full tensor L_n . From these moments, the conductivity σ , thermopower S , and heat conductivity of the electrons κ_e can be calculated as [32]

$$\sigma = e^2 L_0, \quad (2)$$

$$S = \frac{1}{e\theta} \frac{L_1}{L_0}, \quad (3)$$

and

$$\kappa_e = \frac{1}{\theta} \left(L_2 - \frac{L_1^2}{L_0} \right), \quad (4)$$

where e is the electron charge.

A. Keldysh formalism

In the Keldysh formalism, the general transmission function $T(E) = T_{\text{eff}}(E; \Sigma)$ is an effective transmission function, which results from contributions of different origins. The system is divided into three parts, left, center, and right, where the left and right sides serve as semi-infinite leads and the center region serves as scattering region. Certain scattering events can be realized in the Keldysh formalism by placing virtual terminals, which are also known as Büttiker probes [33], in the scattering region. The virtual terminals absorb and reemit electrons with different phases, thus simulating a phase-breaking scattering event [29,33]. Further details of the implementation are documented in our previous paper [10]. The necessary transmission functions are calculated for every possible terminal configuration via a coherent approach at each in-plane \vec{k}_{\parallel} point as

$$T_{XY}(E, \vec{k}_{\parallel}) = \text{Tr}[\underline{\Gamma}_Y(E, \vec{k}_{\parallel}) \underline{G}(E, \vec{k}_{\parallel}) \underline{\Gamma}_X(E, \vec{k}_{\parallel}) \underline{G}^{\dagger}(E, \vec{k}_{\parallel})], \quad (5)$$

where $X, Y \in \mathbf{S} \wedge \{L, R\}$ are virtual terminals or the contacting left (L) and right (R) terminals. \mathbf{S} is the set of all virtual terminals in the scattering region. The matrix $\underline{\Gamma}_{\alpha} = i(\underline{\Sigma}_{\alpha}(E) \underline{L}_{\alpha} - \underline{\Sigma}_{\alpha}^*(E) \underline{L}_{\alpha}) = -2\text{Im} \underline{\Sigma}_{\alpha} \underline{L}_{\alpha} = 2\Sigma_{\alpha} \underline{L}_{\alpha}$ is the broadening function due to self-energy Σ_{α} at site α . The matrix \underline{L}_{α} is 1 only for one site index α and 0 elsewhere. For $\alpha \in \mathbf{S}$, Σ_{α} is the broadening due to scattering. However, Σ_L and Σ_R describe the contact to the semi-infinite leads and are solely given by the lead material. The partial transmissions $T_{XY}(E, \vec{k}_{\parallel})$ are integrated over the in-plane Brillouin zone to obtain $T_{XY}(E)$. From this \vec{k}_{\parallel} integrated partial transmissions

between the terminals, the resulting effective transmission function T_{eff} through the whole system can be calculated as

$$T_{\text{eff}}(E) = T_{LR}(E) + \sum_{\alpha \in \mathbf{S}} \frac{T_{L\alpha}(E) T_{\alpha R}(E)}{S_{\alpha}(E)} + \sum_{\alpha, \beta \in \mathbf{S}}^{\alpha \neq \beta} \frac{T_{L\alpha}(E) T_{\alpha\beta}(E) T_{\beta R}(E)}{S_{\alpha}(E) S_{\beta}(E)} + \dots \quad (6)$$

Here, $S_{\alpha} = T_{L\alpha}(E) + T_{\alpha R}(E) + \sum_{\beta \in \mathbf{S}}^{\beta \neq \alpha} T_{\alpha\beta}(E)$, $\alpha \in \mathbf{S}$ is the renormalization sum of the probability measure. Note that all $T_{XY}(E)$ also depend on all Σ_{α} ($\alpha \in \mathbf{S}$), because the Green's function $G(E, \vec{k}_{\parallel})$ depends on all Σ_{α} ($\alpha \in \mathbf{S}$). Thus, $T_{XY}(E)$ will change even when a Σ_{α} with $\alpha \neq X, Y$ will change. In the following we assume that $\Sigma_{\alpha} \equiv \Sigma \forall \alpha \in \mathbf{S}$. Consequently, we will write the effective transmission as a function of E and Σ , that is $T_{\text{eff}}(E; \Sigma)$.

One has to be careful since, in the Keldysh formalism, the resistance arises not only from scattering but also from the system's contacts to the leads. This contact resistance R_c is due to the contact of an ideal lead to a scattering region, where only a limited number of transport modes per area exist and contribute to the transport of an electron. The scattering part of the resistance R_S is due to scattering alone. While R_S naturally depends on the length of the system and on Σ , R_c does not. R_c solely depends on the type of the contact. Since the two types of resistances form a series circuit and since $R \propto T^{-1}$, the full transmission can be split up as

$$\frac{1}{T_{\text{eff}}(E, \Sigma)} = \frac{1}{T_c(E)} + \frac{1}{T_S(E, \Sigma)}. \quad (7)$$

Here, the contact transmission $T_c(E)$ is the transmission of a system without virtual terminals, and $T_S(E; \Sigma)$ is the contribution due to scattering. T_c is a transmission function that contributes either 0 or 1 at each \vec{k} point for each band and thus is a measure for the number of transport modes. The contribution due to scattering T_S is a probability measure to what extent an electron can traverse the scattering region without being scattered. Thus it is not bounded between 0 and 1. T_S , therefore, can rise to infinity, if no scattering occurs, that is $T_S \rightarrow \infty$ if $\tau \rightarrow \infty$, as it takes infinitely long to scatter. In the Keldysh formalism, the additional contact resistance ensures that the effective transmission function does not rise to infinity.

As depicted schematically in Fig. 1, the influence of the contact resistance is the main contribution for small scattering self-energies Σ (large $1/\Sigma$). The contact resistance limits the transmission function to a constant value. The scattering contribution is rising to infinity as one would expect for decreasing scattering. Increasing the scattering self-energy (reducing $1/\Sigma$), $T_S(E; \Sigma)$ and $T_{\text{eff}}(E; \Sigma)$ start to overlap and this leads to a decreasing contribution of the contact resistance in the reciprocal addition of Eq. (7). Thus in the limit of a very long scattering region or strong scattering, the behavior is of only Ohmic nature and the contact resistance does not contribute significantly. We use the term contact resistance for the resistance, which is due to the contact of semi-infinite leads that serve as an electronic reservoir in equilibrium to a scattering region. Here, we consider no contact resistance from surface roughness, etc., like it would be the case in

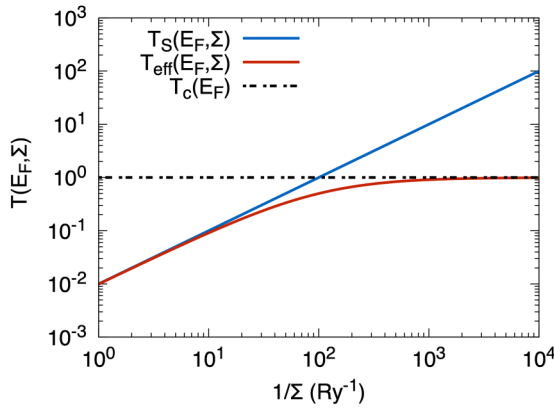


FIG. 1. Schematic depiction of the contributing transmission functions: contact transmission $T_c(E_F)$ (dashed, black), contributions due to scattering $T_S(E_F, \Sigma)$ (blue), and resulting effective transmission $T_{\text{eff}}(E_F, \Sigma)$ (red) via Eq. (7).

experiments. Unless stated otherwise, we consider only the contribution due to scattering $T_S(E; \Sigma)$ in the following as this is the quantity making contact with the Boltzmann approach.

B. Boltzmann formalism

The Boltzmann transmission function contains contributions due to scattering only and no contribution from the contact resistance. The transmission function in the Boltzmann approach corresponds to $T(E, \vec{k}) = T_S(E, \vec{k}; \tau) = v_z^2(\vec{k})\tau_{\vec{k}}\delta(E - \epsilon(\vec{k}))$, where v_z is the group velocity in transport direction, $\tau_{\vec{k}}$ the \vec{k} dependent scattering time, $\delta(E - \epsilon(\vec{k}))$ is the Dirac delta distribution, and $\epsilon(\vec{k})$ is the electronic energy dispersion.

In the case of free electrons, mapping this transmission function onto the \vec{k}_{\parallel} plane, which in accordance to Keldysh is equivalent to integrating the k_z components, one arrives at $T_S(E, \vec{k}_{\parallel}; \tau) = \frac{2\sqrt{2}\tau}{\hbar\sqrt{m}}\sqrt{E - (\hbar^2/(2m))(k_x^2 + k_y^2)}$. Here, we consider the isotropic relaxation time approximation, where τ is independent of \vec{k} [34–38]. Thus, the moments L_n after Eq. (1) are proportional to τ and therefore S is independent of τ . That is $\frac{\partial S}{\partial \tau} = 0$, as seen by Eq. (3). Therefore, scattering has no effect on the thermopower in the Boltzmann approach. Consequently, the thermopower can be used as a theoretical test system of the relation between Σ and τ . Furthermore, if there is a direct relation such as $\tau \propto 1/\Sigma$, the thermopower should be independent of a \vec{k}_{\parallel} -independent self-energy within the Keldysh formalism. In other words, as long as the relation $\Sigma \propto 1/\tau$ holds, the transmission function $T_S(E; \Sigma)$ within the Keldysh approach should linearly depend on $1/\Sigma$, because in the Boltzmann approach the transmission function $T_S(E; \tau)$ is proportional to the relaxation time.

C. Finite differences method

To compare the results obtained with our KKR-Keldysh formalism, we use a three-dimensional finite differences method (FDM) for the system of free electrons. Thereby, we can exclude possible numerical shortcomings in our implementation and more importantly, we can check the

applicability of the virtual terminals in KKR, as we are limited to one virtual terminal at each atom at maximum. In contrast, in FDM the number of virtual terminals is unbound.

For one dimension, the finite differences method (FDM) is described in Ref. [29]. We expand on this description to describe free electrons in three dimensions in an, in principle, exact manner. The Schrödinger equation for free electrons can be separated for each spatial dimension. The Hamiltonian is discretized in transport direction and Fourier transformed in the in-plane direction. The Fourier transformation yields corrections for the in-plane directions converting the three-dimensional problem to an effective one dimensional problem via an effective energy in z direction (transport direction), that is $E_z = E - \frac{\hbar^2}{2m}(k_x^2 + k_y^2)$. The Greens function is calculated for the effective one-dimensional problem at the effective energy for each in-plane \vec{k}_{\parallel} point in the circle described by $\frac{\hbar^2}{2m}(k_x^2 + k_y^2) \leq E$ and integrated over all \vec{k} points. The transmission out of this range is zero. Further details calculating the transmission can be found in Ref. [10].

III. COMPUTATIONAL DETAILS

For evaluation, we consider three different systems. The first system are free electrons serving as a simple model system. The transport parameters of the free electrons are calculated with the DFT-KKR-Keldysh formalism and compared to FDM-Keldysh formalism. As a second system we consider Cu within KKR, because the Fermi surface is very similar to that of free electrons. Finally, as a third system we consider Pd with a rather complex Fermi surface also in KKR.

The potential for the transport calculation in case of free electrons (fe) is a constant potential set to 0. The potentials for Cu and Pd are self-consistently calculated as bulk systems and then used in the transport geometry. Each system is calculated as fcc lattice, where the transport direction is the [001] direction. For the lattice constants we use $a_{\text{fe}} = a_{\text{Cu}} = 6.8311736a_B$, $a_{\text{Pd}} = 7.3524a_B$. Unless stated otherwise, each system has an effective length of $d = 25a_{\text{lat}}$, which means that 50 virtual terminals are placed inside the scattering region. Within the KKR method, the transport calculations are done with 400×400 \vec{k}_{\parallel} points, $\ell_{\text{max}} = 3$, and an energy broadening of 0.054 meV to ensure convergence of $T_S(E; \Sigma)$ to be better than 1%. In FDM we use 2000 lattice points and 400×400 \vec{k}_{\parallel} points for the free electrons to ensure a convergence of $T_S(E; \Sigma)$ better than 1%.

IV. RESULTS AND DISCUSSION

A. KKR results

First in Fig. 2, we compare the thermopower of three different systems with increasing complexity of the Fermi surface, namely free electrons, copper (Cu), and palladium (Pd). We assume a \vec{k} independent scattering time τ and thus use a \vec{k} independent self-energy Σ for the Keldysh formalism with virtual terminals. In this simple case of a constant scattering time approximation, the thermopower generally should show no dependence on τ following the direct linear scaling of the moments L_0 and L_1 with respect to τ

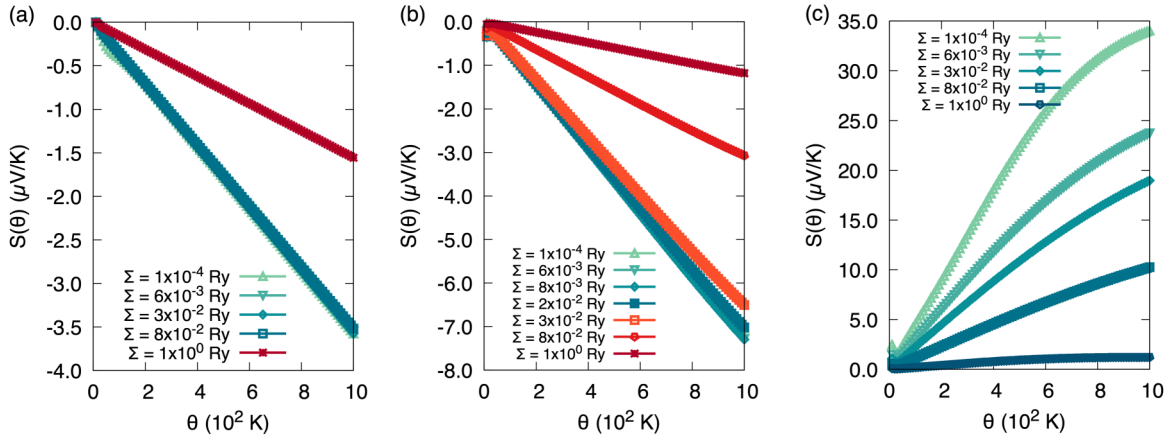


FIG. 2. Thermopower $S(\theta)$ as function of temperature θ for (a) free electrons, (b) Cu, and (c) Pd at different Σ calculated with KKR. Note that in (a) and (b) the blue colored lines overlap.

when considering the Boltzmann theory. If the identification $\tau \propto 1/\Sigma$ is true, it should also give an independence of the thermopower on Σ calculated within the KKR-Keldysh formalism.

1. KKR Thermopower

For free electrons, the thermopower, as a function of temperature θ at an arbitrarily chosen value of $E_F = E_1 = 0.75$ Ry, shows exactly this behavior, at least for Σ roughly below 8×10^{-2} Ry [see Fig. 2(a)]. For higher values of Σ , it starts to deviate (shown in red).

For Cu, shown in Fig. 2(b), the behavior of the thermopower is qualitatively the same as for free electrons. However, the deviation from the expected behavior is already stronger at smaller self-energies Σ compared to free electrons. For Pd, shown in Fig. 2(c), the thermopower shows a distinct temperature dependence for each self-energy, which clearly deviates from the expectation within the relaxation time approximation. This result suggests that a simple identification of $\tau \propto 1/\Sigma$ is not suitable. To get a better understanding we compare the transmission function for these systems in terms of the self-energy. After the comparison of the transmission function, we also check the free electrons against the FDM and discuss the limits of the model in Sec. IV C.

2. KKR Transmission function

In Fig. 3(a) we show the \vec{k}_{\parallel} integrated, energy-dependent transmission function $T_S(E; \Sigma)$ for different scattering self-energies Σ at the Fermi energy for free electrons. At $E_F = E_1 = 0.75$ Ry we find a good linear behavior, especially for high values of $1/\Sigma$, i.e., in the low-scattering regime. This result suggests that for free electrons, the identification of τ with the energy broadening self-energy Σ via $\tau = \frac{\hbar}{2\Sigma}$ is correct at least for small Σ up to around 10^{-1} Ry. But even for free electrons $T_S(E; \Sigma)$ shows deviations from the linear behavior for small values of $1/\Sigma$, i.e., in the case of strong scattering.

This deviation from the linear behavior for large Σ directly relates to the deviation of the thermopower in Fig. 2(a). We attribute the deviation in $T_S(E; \Sigma)$ to an insufficient discretiza-

tion of the scattering events. This will be discussed further in Sec. IV C by means of the FDM.

The same behavior of $T_S(E_F; \Sigma)$ can be observed for Cu in Fig. 3(b). Here, compared to $T_S(E_F; \Sigma)$ of free electrons, the deviation from the linear behavior starts at smaller self-energies already. Again, this deviation is in accordance with the deviation of the thermopower of Cu discussed before.

When considering Pd in Fig. 3(c), with a more complicated electronic structure and complex Fermi surface, the linear fitting of $T_S(E_F, \Sigma)$ in Fig. 3(c) becomes untenable suggesting, that the relationship $\tau \propto 1/\Sigma$ does not hold at all. Again, the complete deviation from the linear behavior is in accordance with the distinct behavior of the thermopower for each self-energy.

So far, we have used the constant scattering time approximation to assess the validity of the identification of $\Sigma = \frac{\hbar}{2\tau}$. For free electrons and Cu, this identification holds true if Σ is small enough, but it is clearly not valid in the case of Pd. The fact that even for simple pure metals in combination with the simple approximation of a constant scattering time [20] the identification of the single-particle scattering time τ and self-energy Σ fails, suggests that for systems with a more complex topology of the Fermi surface and a \vec{k} -dependent scattering time τ , the identification of Σ and τ becomes even more difficult. The main ingredient to the KKR-Keldysh approach is the retarded Green's function defined in the upper half of the complex plane in the limit of real energies. At the real energy axis it possesses poles at the eigenenergies of the eigenstates and each eigenstate is represented by a δ -distribution on the real energy axis. Adding an imaginary part to the real energy causes these states to broaden into a Lorentzian shape. If we consider, as it is the case throughout this paper here, a purely imaginary self-energy of the same value at each atomic site, the real energy and the imaginary self-energy can be seen as a new complex energy, which causes the broadening of the states. This broadening of states, however, causes contributions from neighboring states (neighbors with respect to energy) to an existing state at one particular energy due to the overlap. Also for the transmission at one particular energy, the broadening can cause contributions from neighboring electronic states.

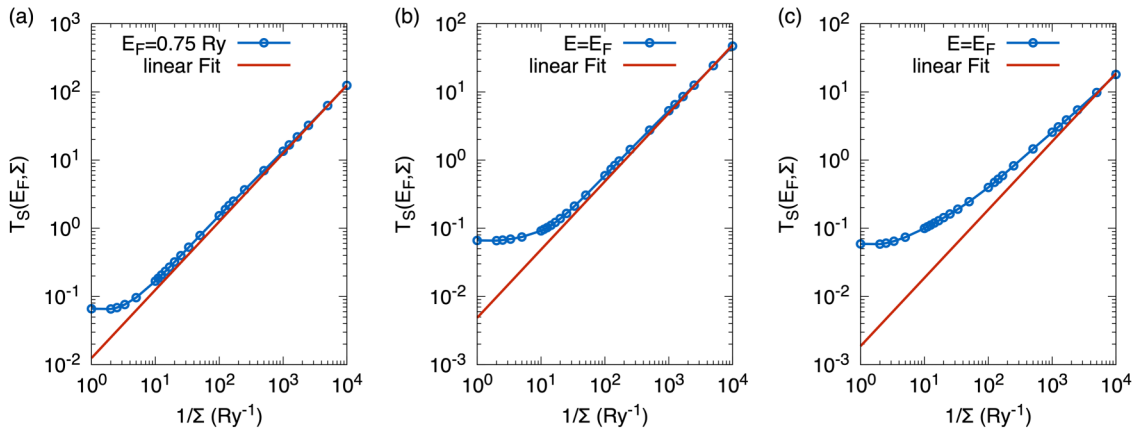


FIG. 3. $T_S(E_F, \Sigma)$ vs $1/\Sigma$ for (a) free electrons, (b) Cu, and (c) Pd in KKR with linear fits.

In the Boltzmann theory, the transport properties at one particular energy are determined solely by the band structure properties of the considered state, and no additional broadening of states is considered. This may cause inaccuracies when translating one quantity into the other and vice versa. Consequently, we attribute the deviations from the linear behavior of Pd to effects caused by the energy broadening.

B. FDM results

In order to test the numerical implementation of the KKR method, we compare it to the thermopower calculated via the FDM method in Fig. 4. We see a similar trend for the deviation of thermopower, namely a deviation of the thermopower for high self-energies. We will explain this deviation for high self-energies in Sec. IV C.

In the Boltzmann approach, considering free electrons, the \vec{k} -integrated $T_S(E; \tau)$ can be shown to be proportional to $\tau E^{3/2}$. The proportionality to $E^{3/2}$ holds true to some extent for the Keldysh version of $T_S(E; \Sigma)$. For comparison, $T_S(E; \Sigma)$ for free electrons is shown in Fig. 5 calculated with FDM and KKR. The transmission functions between the two methods match quite well. In Fig. 6 the \vec{k}_{\parallel} integrated transmission $T_S(E_F; \Sigma)$ is shown for the FDM method for different scattering self-energies Σ . Comparing Fig. 6 with Fig. 3(a) we find for both methods, KKR and FDM, a good linear behavior,

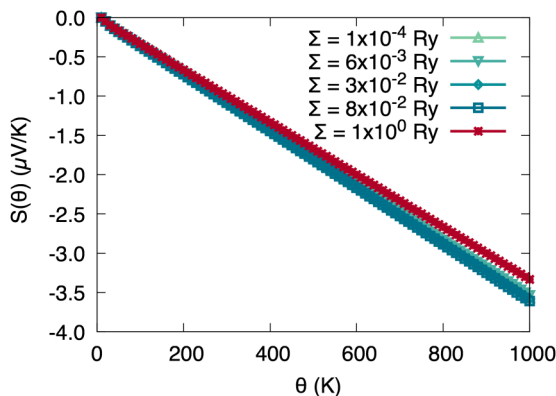


FIG. 4. Thermopower $S(\theta)$ as a function of temperature θ for free electrons calculated with FDM at different Σ .

especially for high values of $1/\Sigma$, i.e., less scattering events. The deviation from the linear behavior appears at smaller self-energies for a lower energy of $E_0 = 0.01$ Ry. While both methods give results that deviate from linear behavior in the strong scattering regime, the precise form is different [cf. Figs. 2(a) and 3(a)]. We discuss this in Sec. IV C. The different characteristic of the deviating thermopower in Figs. 2(a) and 4 are a direct consequence of different deviations of $T_S(E; \Sigma)$ in Figs. 3(a) and 6 in the strong scattering regime.

In the strong scattering regime, both methods overestimate $T_S(E; \Sigma)$ relative to the linear fit. We attribute this to low-energy contributions at the edge of the broadened \vec{k} -dependent transmission. Such a transmission is shown in Fig. 7. In Fig. 7(a) the contact transmission is shown for the first Brillouin zone. The values of $T_c(E_F, \vec{k}_{\parallel})$ are restricted to 1 inside the circle defined by the Fermi energy and 0 outside this circle. The overlapping occurs due to back folding to the Brillouin zone. In Fig. 7(b), the scattering part of the transmission function $T_S(E_F, \vec{k}_{\parallel})$ is shown. The smearing due to scattering at the edges is visible. In Fig. 8, $T_S(E_2; \Sigma)$ at $E_2 = 0.25$ Ry is shown for different integration radii in \vec{k}_{\parallel} space. $T_S(E_2; \Sigma)$ is normalized to the result for $\Sigma = 10^{-4}$ Ry, as the overall area changes for each curve.

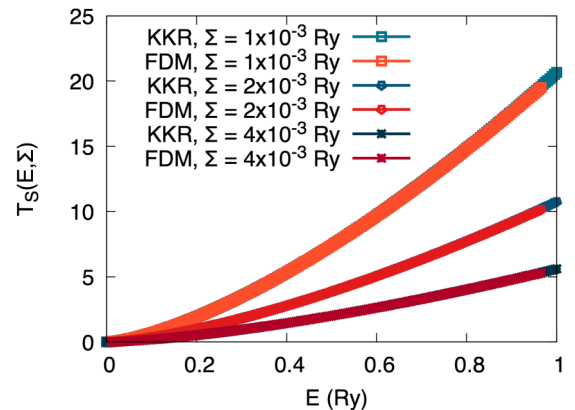


FIG. 5. Scattering contribution to the transmission $T_S(E, \Sigma)$ for different self-energies Σ for free electrons in KKR (blue) and FDM (red).

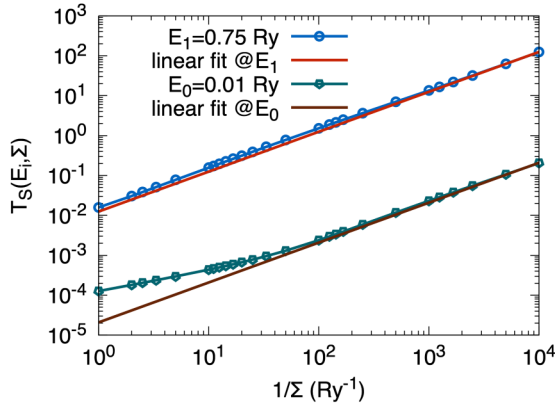


FIG. 6. $T_S(E_i, \Sigma)$, $i = 1, 2$, as function of $1/\Sigma$ for free electrons in FDM with linear fits at $E_0 = 0.01$ Ry and $E_1 = 0.75$ Ry.

At the Γ point, the transmission function shows linear behavior. Integrating only 10% of the radius determined by \sqrt{E} , the behavior stays mostly linear. Integration up to 90% or more shows the deviation from the linear behavior. We attribute this deviation to edge parts of the transmission, where the effective energy for transport in z direction becomes very small such that the discretization of scattering events through the virtual terminals is not sufficient. We elaborate more on this topic in the next section.

C. Limits of the model

Since there are apparent deviations of $T_S(E; \Sigma)$ [see Figs. 3(a) and 6] from the linear behavior, we investigate this problem in terms of the number and placement of virtual terminals. For this we use the FDM model since it provides more freedom to test the placement of virtual terminals compared to the KKR method. In contrast to the continuous FDM or Boltzmann theory, within the KKR framework, the highest possible number of virtual terminals that can be placed in the scattering region is the number of atoms in the cell as the virtual terminals are placed at the atomic positions.

In the FDM model, the space in z direction is discretized. The corresponding discretization parameter $a = d_z/(n - 1)$

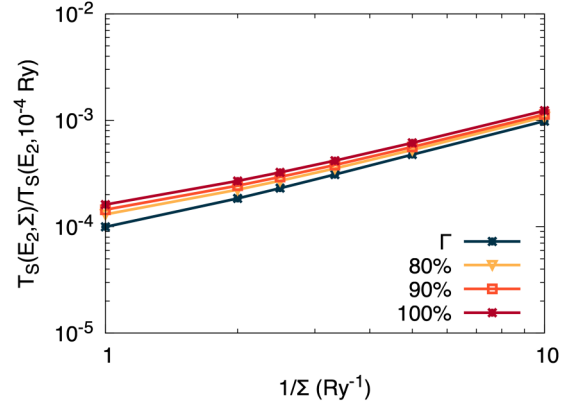


FIG. 8. Normalized transmission function $T_S(E_2; \Sigma)/T_S(E_2; 10^{-4} \text{ Ry})$ of free electrons calculated with FDM at $E_2 = 0.25$ Ry. $T_S(E_2, \Sigma)$ shows linear behavior at the Γ point (blue). Integrating up to 80%, 90%, and 100% (warm colors) of the radius of the broadened transmission circle \vec{k}_{\parallel} space shows overestimations from the expected linear behavior.

can be chosen arbitrarily small in principle and must be chosen reasonably small to achieve convergence for the effective transmission. On each of these n discretized lattice points, it is possible to place a virtual terminal.

Figure 9 shows $\Delta T_S/T_S$ for $E_0 = 0.01$ Ry and $E_1 = 0.75$ Ry (blue, red), respectively, for different values of Σ . Starting from 2000 lattice points, a virtual terminal is located at every lattice point. To test the discretization of the scattering events, we reduce the number of virtual terminals. The placement is uniform such that a virtual terminal is added to every i th lattice point. To achieve the same total amount of scattering, the self-energy Σ_i of the i th individual virtual terminal is scaled so that the sum $\sum_{i \in S} \Sigma_i$ stays constant. The actual number of virtual terminals is shown on the x axis.

With this test, it is possible to show that for a certain number of virtual terminals at a certain self-energy Σ , the obtained result for $T_S(E_i; \Sigma)$ deviates significantly from the value of $T_S(E_i; \Sigma)$ when it is discretized to the maximum at 2000 lattice points. The deviation increases as the number of virtual terminals decreases, going beyond 1% for less

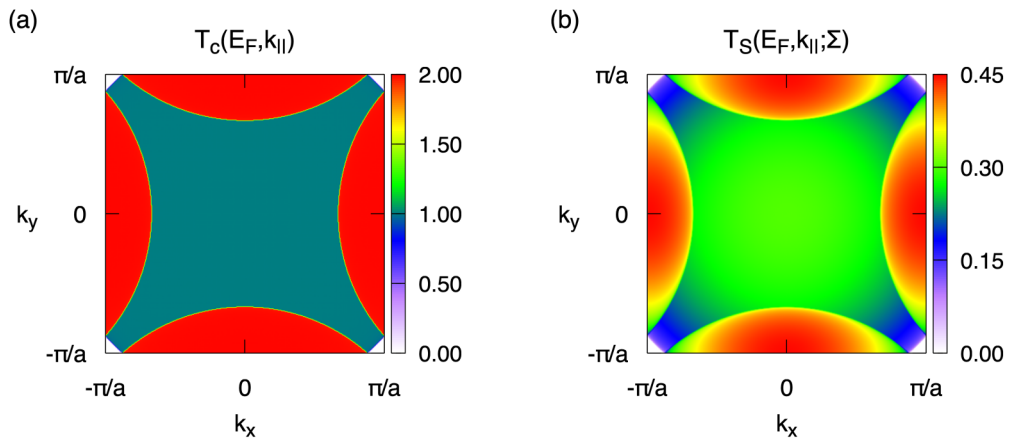


FIG. 7. \vec{k}_{\parallel} -dependent transmission function of free electrons calculated with KKR. (a) Contact transmission function and (b) scattering part of transmission $T_S(E_F, \vec{k}_{\parallel}, \Sigma)$ for $\Sigma = 3 \times 10^{-2}$ Ry.

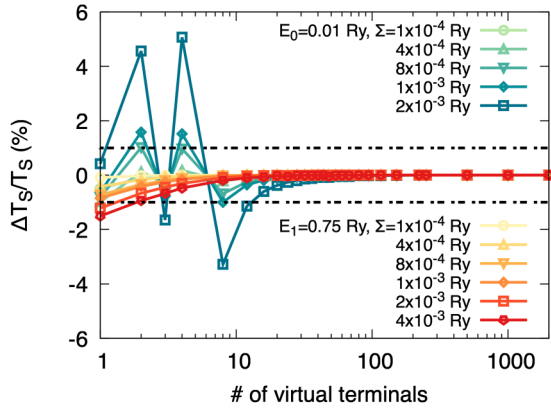


FIG. 9. Relative deviation of $T_S(E_i, \Sigma)$ vs number of virtual terminals for free electrons. As the number of virtual terminals inside the constant scattering region decreases, the distance between the virtual terminals increases. The single Σ_i has to be scaled accordingly, to meet the condition $\sum_{i \in S} \Sigma_i = \text{const.}$

than about 10 terminals for $E = 0.01$ Ry. We attribute this to multiple-scattering effects with a very high number of scattering events that cannot be accounted for due to the lack of the necessary number of virtual terminals. Thus, the discretization to describe all scattering events is insufficient.

For larger Σ or smaller E this starts to happen for a higher number of virtual terminals, i.e., a finer discretization, as the number of scattering events, that should occur is antiproportional to the mean free path $\lambda = v\tau = \sqrt{2E/m} \hbar / (2\Sigma)$. Transferring this result to the KKR method implies that at very high self-energies, the discretization of the scattering events is not sufficient anymore. Thus, interatomic positions for virtual terminals would have to be utilized to overcome this deficiency.

To test whether this effect is related to the actual distance of virtual terminals, we randomly placed 20 virtual terminals in the transport cell. Figure 10 shows $\Delta T_S / T_S$ for different random distributions of virtual terminals. For larger self-energies, some distributions show larger deviations. The results suggest that virtual terminals can actually be placed randomly but yield the same result within 1% deviation as long as the

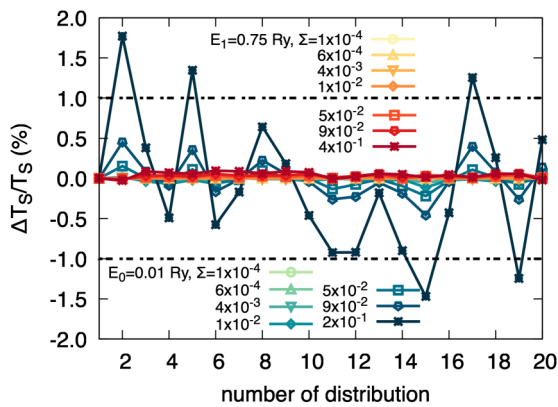


FIG. 10. Relative deviation of $T_S(E_i, \Sigma)$ for free electrons vs 20 different distributions of a constant number of 20 virtual terminals, which are placed randomly over the scattering region.

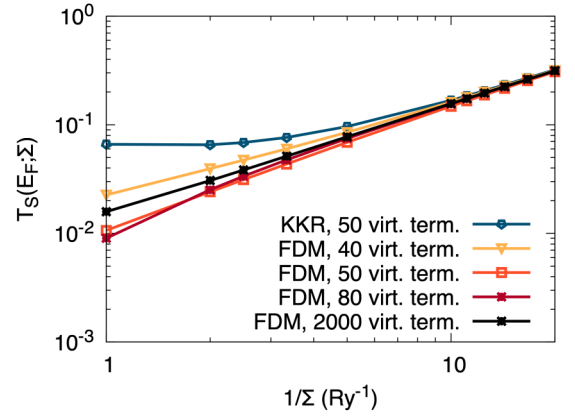


FIG. 11. $T_S(E_F, \Sigma)$ vs $1/\Sigma$ for free electrons for different discretizations of the scattering potential barrier. The actually used self-energy Σ' has to be scaled to meet the “effective” self-energy Σ .

self-energy is small enough for the scattering events to be accounted for. This means that the effective strength of the scattering region is not determined by the region covered with virtual terminals but only by the overall strength of self-energies $\sum_{i \in S} \Sigma_i$. The distance between the virtual terminals is not crucial since the transmission between two terminals $T_{\alpha\beta}$ is calculated coherently. With these restrictions in mind, a description of a macroscopic experimental thin film should be possible. The practical route is to calculate a microscopic, downsized version of the thin film. In order to account for the same scattering strength, the self-energies have to be scaled according to the length of the scattering region. Here it is crucial to introduce a sufficient number of virtual terminals to account for all necessary multiple scattering events.

Finally, let us explain the observed deviation of $T_S(E_F, \Sigma)$ for large self-energies in the KKR approach. In Fig. 11, $T_S(E_F, \Sigma)$ for the KKR method, where a virtual terminal is attributed to each atomic position is compared to the FDM method with a changing number of virtual terminals. The FDM method for 2000 virtual terminals is considered as the exact converged result. Depending on the number of virtual terminals, $T_S(E_F; \Sigma)$ over- or underestimates the correct result in the strong scattering regime. Additionally, since the KKR uses different approximations than the FDM, e.g., atomic sphere potentials and expansion of functions in spherical harmonics with ℓ cutoffs, deviations are expected to occur, while not necessarily with the same numerical value.

V. CONCLUSION

We calculated the thermopower $S(\theta)$ and the transmission function $T_S(E; \Sigma)$ for free electrons, Cu, and Pd with scattering events realized by virtual terminals. The thermopower $S(\theta)$ for the free electrons and Cu shows no dependence on the self-energy Σ , if it is below a specific value of Σ . This is directly related to the linear scaling of $T_S(E; \Sigma)$ with $1/\Sigma$ in that regime for the two systems. For free electrons, we can explain the deviations from the linear behavior in terms of insufficient discretization of scattering events. Further, we show that the distance between virtual terminals plays no

role, as long as enough scattering events are considered. For Pd, however, we find a nonlinear behavior in $T_S(E; \Sigma)$ even for small self-energies Σ and a distinct behavior of the thermopower $S(\theta)$ for each self-energy Σ . This result suggests that τ may not be easily identified with $\hbar/(2\Sigma)$ for more complex Fermi surfaces. We conclude that even in the simple constant relaxation time approximation with \vec{k} -independent τ the identification of the scattering time with the lifetime associated with \vec{k} -independent Σ is not true in general. For the case of a \vec{k} -dependent τ or the energy-dependent self-energy function $\Sigma(E)$ obtained from rigorous many-body treatment, this identification would become even more problematic. We have shown possible errors in the KKR approach when using virtual terminals to describe scattering, namely using too large self-energies, and low-energy contributions at the edge of the Fermi surface. These errors however, are very small when considering practical self-energies for Cu and Pd. For Cu, values for Σ ranging from $7 \times 10^{-4} - 3.7 \times 10^{-3}$ Ry were calculated [39] in good agreement with the referenced experiment therein. For Pd, values ranging from $3.7 \times 10^{-4} - 1.1 \times 10^{-2}$ Ry were calculated depending on temperature and

surface state [40,41]. Considering the limits of the virtual terminal approach, it should be possible to calculate macroscopic thin films, which opens up the way to describe real experimental structures. As we have shown in an earlier paper [42] that it is possible to calculate the spin accumulation in clean systems within the Keldysh formalism, extending it to scattering via virtual terminals could make it possible to also calculate the spin diffusion length for such systems or to consider additional contributions to the accumulation.

ACKNOWLEDGMENTS

A.F., M.C., and C.H. acknowledge computational resources provided by the HPC Core Facility and the HRZ of the Justus-Liebig-University Giessen. Further, they would like to thank M. Giar and P. Risius of HPC-Hessen, funded by the State Ministry of Higher Education, Research and the Arts, for technical support. M.G. thanks the visiting professorship program of the Centre for Dynamics and Topology at Johannes Gutenberg-University Mainz.

-
- [1] S. Datta and M. J. McLennan, *Rep. Prog. Phys.* **53**, 1003 (1990).
 [2] T. J. Thornton, *Rep. Prog. Phys.* **58**, 311 (1995).
 [3] M. P. Das and F. Green, *J. Phys.: Condens. Matter* **21**, 101001 (2009).
 [4] L. L. Sohn, L. P. Kouwenhoven, and G. Schön (eds.), *Mesoscopic Electron Transport* (Springer Netherlands, Dordrecht, 1997).
 [5] R. Kubo, *J. Phys. Soc. Jpn.* **12**, 570 (1957).
 [6] T. Low, A. S. Rodin, A. Carvalho, Y. Jiang, H. Wang, F. Xia, and A. H. Castro Neto, *Phys. Rev. B* **90**, 075434 (2014).
 [7] S. Lowtizer, M. Gradhand, D. Ködderitzsch, D. V. Fedorov, I. Mertig, and H. Ebert, *Phys. Rev. Lett.* **106**, 056601 (2011).
 [8] G. Y. Guo, Y. Yao, and Q. Niu, *Phys. Rev. Lett.* **94**, 226601 (2005).
 [9] Y. Yao and Z. Fang, *Phys. Rev. Lett.* **95**, 156601 (2005).
 [10] C. E. Mahr, M. Czerner, and C. Heiliger, *Phys. Rev. B* **96**, 165121 (2017).
 [11] C. Heiliger, M. Czerner, B. Y. Yavorsky, I. Mertig, and M. D. Stiles, *J. Appl. Phys.* **103**, 07A709 (2008).
 [12] C. Franz, M. Czerner, and C. Heiliger, *J. Phys.: Condens. Matter* **25**, 425301 (2013).
 [13] I. Mertig, *Rep. Prog. Phys.* **62**, 237 (1999).
 [14] W. Li, *Phys. Rev. B* **92**, 075405 (2015).
 [15] J. M. Ziman, *Principles of the Theory of Solids*, 2nd ed. (Cambridge University Press, Cambridge, 1972).
 [16] C. Herschbach, M. Gradhand, D. V. Fedorov, and I. Mertig, *Phys. Rev. B* **85**, 195133 (2012).
 [17] G. Géranton, B. Zimmermann, N. H. Long, P. Mavropoulos, S. Blügel, F. Freimuth, and Y. Mokrousov, *Phys. Rev. B* **93**, 224420 (2016).
 [18] J. K. Glasbrenner, B. S. Pujari, and K. D. Belashchenko, *Phys. Rev. B* **89**, 174408 (2014).
 [19] A. A. Starikov, Y. Liu, Z. Yuan, and P. J. Kelly, *Phys. Rev. B* **97**, 214415 (2018).
 [20] R. Golizadeh-Mojarad and S. Datta, *Phys. Rev. B* **75**, 081301(R) (2007).
 [21] C.-L. Chen, C.-R. Chang, and B. K. Nikolić, *Phys. Rev. B* **85**, 155414 (2012).
 [22] M. Calandra and F. Mauri, *Phys. Rev. B* **76**, 205411 (2007).
 [23] M. Sentef, A. F. Kemper, B. Moritz, J. K. Freericks, Z.-X. Shen, and T. P. Devereaux, *Phys. Rev. X* **3**, 041033 (2013).
 [24] A. F. Kemper, O. Abdurazakov, and J. K. Freericks, *Phys. Rev. X* **8**, 041009 (2018).
 [25] S.-L. Yang, J. A. Sobota, D. Leuenberger, Y. He, M. Hashimoto, D. H. Lu, H. Eisaki, P. S. Kirchmann, and Z.-X. Shen, *Phys. Rev. Lett.* **114**, 247001 (2015).
 [26] K. Sugawara, T. Sato, S. Souma, T. Takahashi, and H. Suematsu, *Phys. Rev. Lett.* **98**, 036801 (2007).
 [27] G. Moos, C. Gahl, R. Fasel, M. Wolf, and T. Hertel, *Phys. Rev. Lett.* **87**, 267402 (2001).
 [28] I. Gierz, S. Link, U. Starke, and A. Cavalleri, *Faraday Discuss.* **171**, 311 (2014).
 [29] S. Datta, *Electronic Transport in Mesoscopic Systems* (Cambridge University Press, Cambridge, 1995).
 [30] J. Zabloudil, ed., *Electron Scattering in Solid Matter: A Theoretical and Computational Treatise*, Springer Series in Solid-State Sciences No. 147 (Springer, Berlin, 2005).
 [31] M. Czerner and C. Heiliger, *J. Appl. Phys.* **111**, 07C511 (2012).
 [32] Y. Ouyang and J. Guo, *Appl. Phys. Lett.* **94**, 263107 (2009).
 [33] M. Büttiker, *Phys. Rev. B* **32**, 1846 (1985).
 [34] D. I. Pikulin, C.-Y. Hou, and C. W. J. Beenakker, *Phys. Rev. B* **84**, 035133 (2011).
 [35] M. Zebarjadi, S. E. Rezaei, M. S. Akhanda, and K. Esfarjani, *Phys. Rev. B* **103**, 144404 (2021).
 [36] A. Hackl and S. Sachdev, *Phys. Rev. B* **79**, 235124 (2009).
 [37] C. Zhang, S. Tewari, and S. Chakravarty, *Phys. Rev. B* **81**, 104517 (2010).
 [38] L. Chaput, P. Pécheur, and H. Scherrer, *Phys. Rev. B* **75**, 045116 (2007).

- [39] M. Xu, J.-Y. Yang, S. Zhang, and L. Liu, [Phys. Rev. B **96**, 115154 \(2017\)](#).
- [40] I. Y. Sklyadneva, A. Leonardo, P. M. Echenique, S. V. Eremeev, and E. V. Chulkov, [J. Phys.: Condens. Matter **18**, 7923 \(2006\)](#).
- [41] I. Y. Sklyadneva, R. Heid, V. M. Silkin, A. Melzer, K. P. Bohnen, P. M. Echenique, T. Fauster, and E. V. Chulkov, [Phys. Rev. B **80**, 045429 \(2009\)](#).
- [42] A. Fabian, M. Czerner, C. Heiliger, H. Rossignol, M.-H. Wu, and M. Gradhand, [Phys. Rev. B **104**, 054402 \(2021\)](#).